THE JOURNAL OF PHYSICAL CHEMISTRY C
Article
pubs.acs.org/JPCC

High Heating Rate Reaction Dynamics of Al/CuO Nanolaminates by Nanocalorimetry-Coupled Time-of-Flight Mass Spectrometry

Jeffery B. DeLisio,[†,§] Feng Yi,[‡,§] David A. LaVan,[*,‡] and Michael R. Zachariah[*,†]

[†]Department of Chemistry and Biochemistry, and Department of Chemical and Biomolecular Engineering, University of Maryland, College Park, Maryland 20742, United States

[‡]Materials Measurement Science Division, Material Measurement Laboratory, National Institute of Standards and Technology, Gaithersburg, Maryland 20899, United States

Supporting Information

ABSTRACT: Highly tunable reactive nanolaminates have been of recent interest for various "on chip" energetic applications. The reaction dynamics of Al/CuO nanolaminates were investigated by nanocalorimetry-coupled time-of-flight mass spectrometry, capable of simultaneous measurement of temporal thermal dynamics and detection of evolved gas phase species at heating rates up to ~10^6 K/s. The nanolaminates were synthesized by alternately sputtering Al and CuO onto the heater of nanocalorimeter sensors. For thin films of 80 nm with one bilayer, the stoichiometric ratio of fuel to oxidizer significantly affected the reaction mechanism: initial reactions occurred between 300 and 400 °C, and main reactions varied based on stoichiometry. For thicker films of 199 and 266 nm, a series of samples with varying bilayer numbers were analyzed to determine the effect of diffusion distance and interfacial area. Only one reaction step was observed for a sample with a bilayer thickness of 33 nm. A two-step reaction mechanism is observed as the bilayer thickness was increased to 66 nm and beyond: solid-state reaction occurring at the interfaces of Al and CuO before the melting of Al and a much faster liquid−solid reaction right after the melting of Al. At the same time, interfacial premixed distance during the deposition was also estimated from parallel experiments. Furthermore, the power data from nanocalorimetry provides a more direct method, compared to optical emission and mass spectrometry based methods, in determining the ignition temperature in addition to being able to measure actual energy output for films with nanoscale thicknesses.

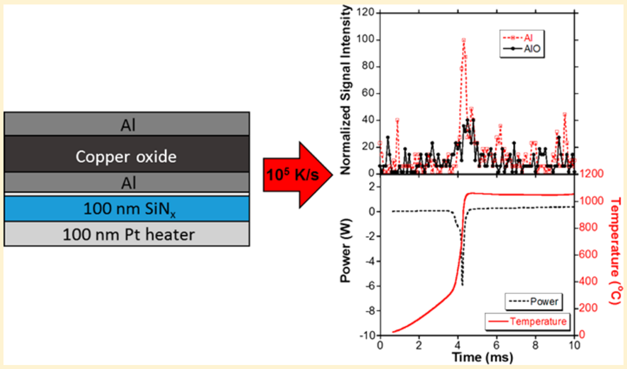

INTRODUCTION

Energetic nanocomposites have been of recent interest for a wide variety of applications due to their high volumetric energy densities, relatively fast reaction kinetics, and decreased ignition temperatures.[1−3] The enhancements gained when using nanosized components, as opposed to micron-sized particles, are due to increased interfacial area and decreased diffusion length scales. These systems are typically composed of a metal fuel, most commonly aluminum (Al), and a metal oxide oxidizer. Energetic nanocomposites can be manufactured with a wide range of architectures ranging from physical mixtures of nanosized particles to sputter deposited multilayered nanofoils, often referred to as nanolaminates.[4,5]

Nanolaminates, in particular, have various uses in microelectromechanical systems (MEMS), microelectronics, and material bonding applications.[6−10] The simple geometry at the fuel/oxidizer interface of multilayered laminates also provides an ideal system to further study the oxygen transport in thermite based reactions, making it possible to probe factors such as the influence of interface-to-volume ratio and its effect on ignition and energy release. These systems can have very low ignition temperatures (below the melting point of Al) and enhanced reactivity based on the number of bilayers.[11,12]

The reaction dynamics of energetic nanolaminates have been extensively studied at relatively slow heating rates (~10 K/min) using differential scanning calorimetry and thermogravimetric analysis.[11,13,14] A recent study by Egan et al. used high heating rate analytics, which more accurately represent the time scales of a combustion event, to determine the effect of bilayer thickness on the reaction mechanism of Al/CuO nanolaminates.[12] Egan et al. used temperature jump (T-jump) time-of-flight mass spectrometry (ToF-MS) coupled with high speed videography to measure the ignition temperature of 1−12 bilayer nanolaminates with a fixed total thickness.

In this work, the reaction dynamics of the Al/CuO nanolaminate system was further studied by replacing the T-jump ignition system with a chip based nanocalorimeter capable of collecting thermal data while heating at rates of up to

Received: November 4, 2016
Revised: January 5, 2017
Published: January 7, 2017

DOI: 10.1021/acs.jpcc.6b11114
J. Phys. Chem. C 2017, 121, 2771−2777

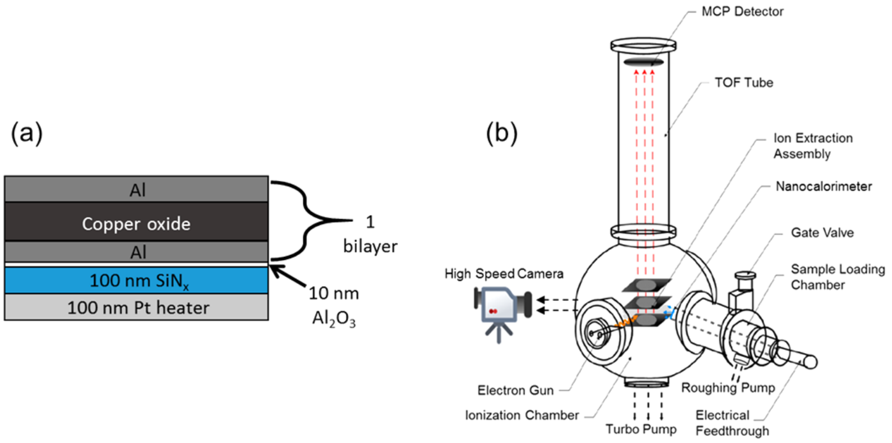

Figure 1. Diagram of sputter deposited single bilayer Al/CuO nanolaminate (a) and ToF-MS experimental setup with integrated nanocalorimeter and high speed imaging (b).

~10^6 K/s.[15] The integration of nanocalorimetry with ToF-MS allows for simultaneous temporal thermal and speciation measurement.[16] The incorporation of the nanocalorimeter also allows for the study of Al/CuO nanolaminates with significantly thinner bilayers than those previously studied, which do not visibly show ignition occurring. We report the effects of stoichiometry, total thickness, and individual bilayer thickness on the reaction mechanism of Al/CuO nanolaminates in addition to providing a more accurate method to determine the ignition temperature of these systems.

EXPERIMENTAL SECTION

Sample Preparation. The Al/CuO laminates were prepared using sputter deposition techniques. The Al and CuO sputter targets were purchased from Kurt Lesker, and the CuO target was indium bound to a copper backing plate for better heat dissipation during the sputtering. A DC power of 300 W is used for aluminum sputtering, and a RF power of 300 W is used for CuO sputtering. The sputtering was performed under a pressure of 0.67 Pa of argon. During deposition, the target not in use was turned off to prevent contamination. XRD analysis (Figure S1) was performed on a sputter deposited pure CuO film to verify the composition. The nanocalorimeter sensor has a 100 nm-thick platinum heater suspended on a 100 nm-thick silicon nitride membrane in a silicon frame. The samples are deposited on the silicon nitride side of the nanocalorimeter sensor. As shown in Figure 1, 10 nm of alumina was deposited using atomic layer deposition to serve as a barrier layer between the sample and sensor. The first and last layer deposited was aluminum so that one bilayer is defined as two "half" layers of aluminum and one layer of copper oxide as shown in Figure 1a. Sample thicknesses, bilayer thickness, and stoichiometry of the laminate were varied to investigate the reaction dynamics of Al/CuO nanolaminates.

Nanocalorimetry Measurements. The nanocalorimetry system can measure a thermal signal at heating rates up to 10^6 K/s. The calibration of the nanocalorimeter sensors used in this work has been previously described in detail.[17] Briefly, the resistance and temperature were recorded by electrical measurements and an optical pyrometer during the resistive heating/cooling. In order to calculate enthalpy, a previously published method[18] was used that entailed heating each empty nanocalorimeter sensor at various heating rates to determine the heat losses and heat capacity of the bare sensor. The power associated with the sample could then be calculated from the total power by subtracting the power associated with the bare sensor and the heat losses. Optical emission from the chip during heating was also recorded using a high speed camera (Phantom v12.0, 67,000 frames per second), but that data is not part of the nanocalorimeter measurement.

Time-of-Flight Mass Spectrometer System. A previously reported technique describes the integration of the nanocalorimeter into a time-of-flight mass spectrometer (ToF-MS).[16] Figure 1b shows a diagram of the integrated setup with high speed videography to record optical emission from reaction. Specific details of the linear ToF-MS system used for this study have been previously reported.[19,20] The nanocalorimeter sensor was inserted into the ionization region of the ToF-MS using a linear motion feedthrough with a 3D printed adapter and sensor cover. A sampling rate of 100 μs per spectrum (10 kHz) was used to capture the progress of the reaction with 100 spectra obtained post-triggering for each run. Gas phase reaction products were ionized for 3 μs using an electron gun operated at 70 eV and 1 mA. The data was captured and processed using a 600 MHz digital oscilloscope.

RESULTS

Effect of Stoichiometry on Al/CuO Reaction. In order to first evaluate the effect of stoichiometry on the reaction mechanism, films of varying equivalence ratios (ϕ) were rapidly heated on the nanocalorimeter within the ionization region of the ToF-MS. Figure 2 shows the nanocalorimetry results from rapid heating (~10^5 K/s) of the respective Al/CuO nanolaminates. These samples each have only one bilayer. The ratio of Al:CuO was varied, and the total thickness was kept constant at 80 nm. All three samples show an initial exothermic peak with an onset temperature between 300 and 400 °C. The thermal data was much clearer for the fuel-rich sample with the predominant exotherm occurring at the melting point of Al. The third exothermic reaction occurred around the decomposition temperature of CuO. This sample was run a second time (Figure S2), and a sharp endotherm was detected corresponding to the Al–Cu eutectic. As the equivalence ratio reduced to 1, the stoichiometric ratio, the main reaction exotherm was shifted to a higher temperature closer to the decomposition of CuO. This may be related to the diffusivity of liquid aluminum. The main exothermic peak becomes much broader in the fuel-lean sample and spans from the melting

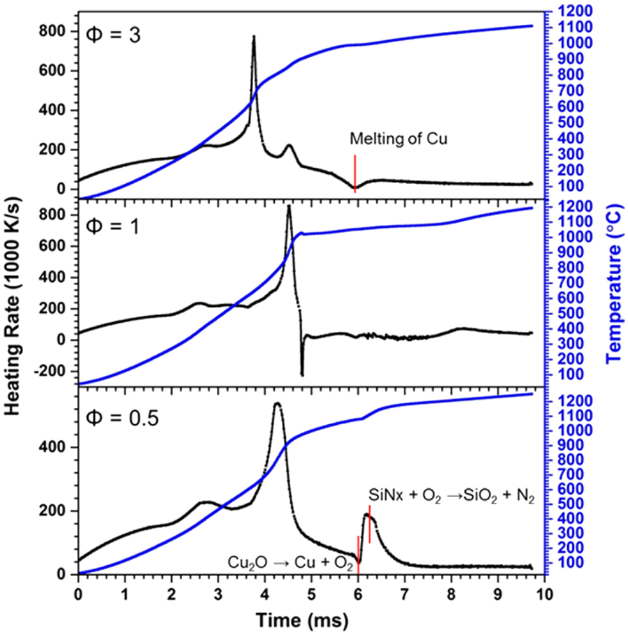

Figure 2. Heating rate and temperature vs time plots for 80 nm-thick, one-bilayer Al/CuO nanolaminates with equivalence ratios (ϕ) of 0.5, 1, and 3.

point of Al to the decomposition temperature of CuO. An endothermic reaction is observed that occurs after the Al/CuO reaction and corresponds to the decomposition of Cu_2O to Cu and O_2. At these temperatures, the generated O_2 can react with the SiN_x on the chip to produce SiO_2 and N_2, which will be addressed in more detail in a parallel paper.

Effect of Total Sample Thickness and Bilayer Number. The aforementioned samples with total thicknesses of 80 nm did not produce sufficient gas phase reaction products for detection in the ToF-MS. In addition, previous work done investigating particulate based Al/CuO nanothermites using the T-jump ToF-MS system demonstrated that fuel-rich samples showed increased signal intensities for Al containing reaction intermediates in the MS.[20] A series of thicker, fuel-rich samples (ϕ = 1.5) were tested with total thicknesses of 199 and 266 nm with varying bilayer number and thickness as seen in Table 1. For each of the samples listed in Table 1, two nanocalorimeter chips were prepared to ensure repeatability of the results.

Table 1. Sample Thickness, Bilayer Number, and Bilayer Thickness for Each of the Studied Al/CuO Nanolaminate Samples

sample ID	sample thickness (nm)	bilayer number	bilayer thickness (nm)
A	199	6	33
B	199	3	66
C	266	4	66
D	266	2	133

Optical emission for each of these samples varied depending on the total thickness and number of bilayers. All samples besides sample A showed visible signs of ignition (Figure S3) in the captured high speed video. We propose that for these nanolaminates there is a threshold for visible ignition to occur, which is determined by the amount of active material in the system. Samples A and B have the same total thickness, yet sample A has double the number of bilayers resulting in a lower active material content possibly due to the presence of more premixed regions. This will be discussed in detail below.

Figure 3 shows the time-resolved Al and AlO release, temperature, and power results for the 199 nm total thickness Al/CuO nanolaminates.

The MS results are normalized to the maximum Al signal intensity. Previous T-jump ToF-MS experiments have shown the detection of Al in the MS at ~1450 °C during rapid heating of Al nanoparticles.[20] For the Al/CuO nanolaminates, Al is detected at a much lower temperature due to the rapid reaction between Al and CuO. For samples A and B, the Al signal peak intensity occurs at the same point as the maximum power shown in the nanocalorimetry data.

The ratio of AlO to Al signal intensity is much larger in the six-bilayer system (Figure 3A) in comparison to the three-bilayer system (Figure 3B). The absolute signal intensity for the Al and AlO peak in the six-bilayer system was 83% and 149% of that for the three-bilayer system further demonstrating the decrease in Al and increase in AlO when more-bilayers are present. In addition, the peak for the AlO signal over time is much sharper in the six-bilayer system. As a control experiment, fully reacted films and pure Al_2O_3 runs were performed, and no Al or AlO species were detected supporting the claim that these species are released during the reaction of the nanolaminate. We propose that the increased interfacial area in the six-bilayer sample results in a faster bulk reaction rate, as seen by the higher maximum power. The increased interfacial area also results in a lower relative Al signal intensity due to the formation of more AlO. The six-bilayer sample has more interfacial area for Al to react as gas phase Al is generated.

Figure 4 shows the ToF-MS and nanocalorimeter results for nanolaminates with a total thickness of 266 nm.

The two-bilayer, 266 nm total thickness sample (D) had the largest individual bilayer thickness of the samples examined in this study. This sample also showed a sharp endothermic peak associated with the melting of excess aluminum at ~4.5 ms. The time-resolved MS data shows a delay in peak Al signal intensity in comparison to the peak AlO signal for the two-bilayer system. This occurs because the two-bilayer sample has more "bulk" aluminum, which slows down the heating rate at the melting point of Al as shown by the sharp endotherm at ~4.5 ms in Figure 4D. The Al located in the center of each individual Al layer must first melt before it can diffuse outward to come in contact with a reactive interface. Once the Al is mobile, the heating rate sharply increases, in turn, resulting in an increase in the Al signal intensity in the MS. The AlO signal intensity is not tied directly to the heating rate as this species will continue to be generated at the reaction interface, even during the endothermic "bulk" Al melting event at ~4.5 ms in Figure 4D. It is also important to note that there is no gas phase O_2 generation visible in the MS for all four samples. This implies a purely condensed phase oxygen transport mechanism occurring before the decomposition temperature of CuO.

Enthalpy of Reaction. Figures 3 and 4 show the resultant power curves for samples A–D along with their respective temporal temperatures. Reaction enthalpies for each sample were calculated by integrating the power during the time of reaction. Because the samples are fuel rich, the experimental enthalpies were normalized with respect to the limiting reagent (CuO) and are listed in Table 2.

Sample A had the lowest experimental enthalpy because this sample has the most bilayers, and in turn, the most premixed regions. Samples B and C had approximately the same

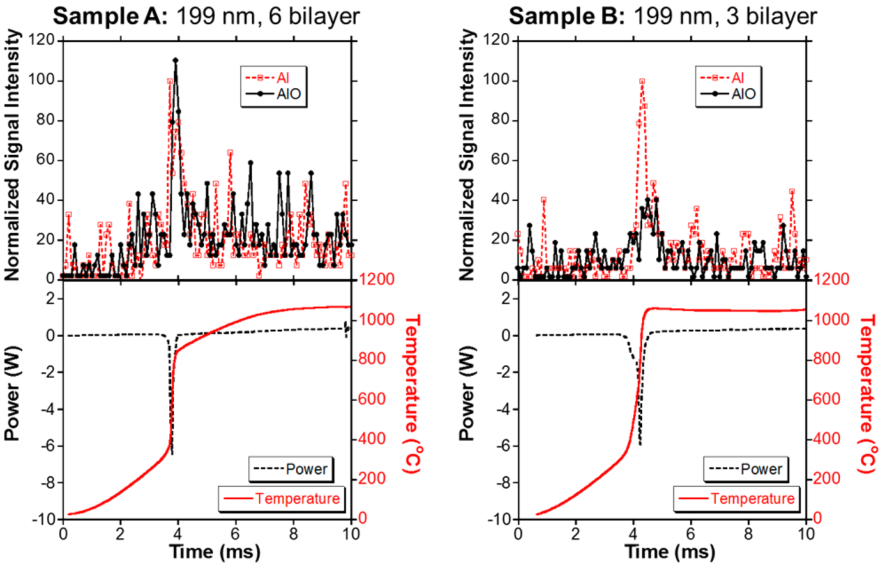

Figure 3. Time-resolved MS and nanocalorimeter results for samples A and B.

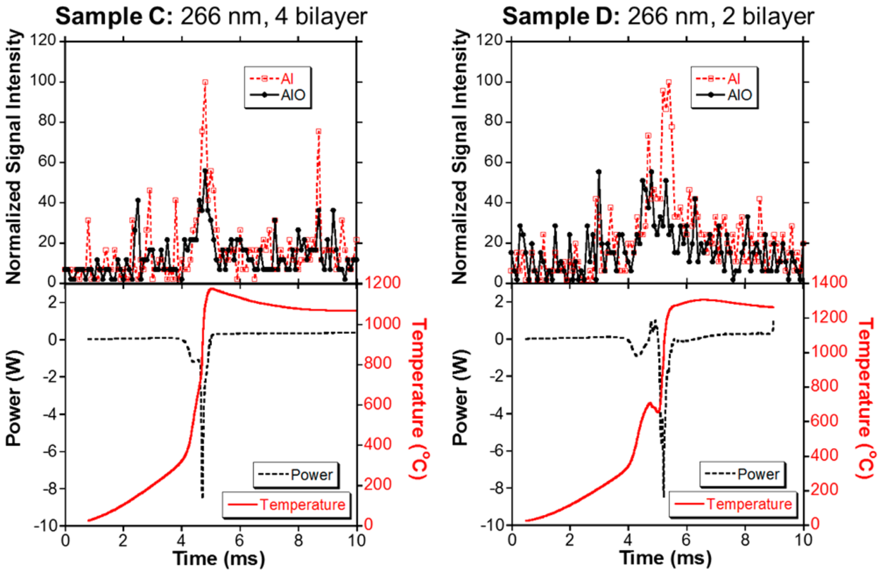

Figure 4. Time-resolved MS and nanocalorimeter results for samples C and D.

Table 2. Experimental Enthalpy of Reactions from Integrated Power vs. Time Curves for Each Sample and Calculated Interface Thickness and Absolute Enthalpy of Reaction

sample ID	sample thickness (nm)	bilayer number	bilayer thickness (nm)	ΔH_{exp} (kJ/mol CuO)	premixed interface thickness (nm)	efficiency factor n
A	199	6	3	−50.3 ± 1.0	9.3 ± 0.1	0.31 ± 0.01
B	199	3	66	−82.4 ± 2.1		
C	266	4	66	−80.3 ± 0.3		
D	266	2	133	−105.7 ± 14		

individual bilayer thickness and also relatively similar experimental enthalpies. Sample D contained the most active material resulting in the largest measured reaction enthalpy. Thus, while more bilayers result in faster energy release, this occurs with a loss of energy density.

One source for potential error in our experimental energy calculation is active Al being lost during rapid heating, as detected by the gas phase Al signal in the MS. The amount of gas phase Al could potentially be much greater in the scope of our experiment when compared to traditional DSC experiments due to the much higher heating rates employed. Additionally, in order to calculate the amount of CuO in each film, a uniform thickness was assumed. One source of error in regards to the normalization of results is the film not having a uniform thickness.

DISCUSSION

Premixed Interfaces. Increasing the number of bilayers was shown to decrease the energy output from the Al/CuO nanolaminates in this study. The following equation was used

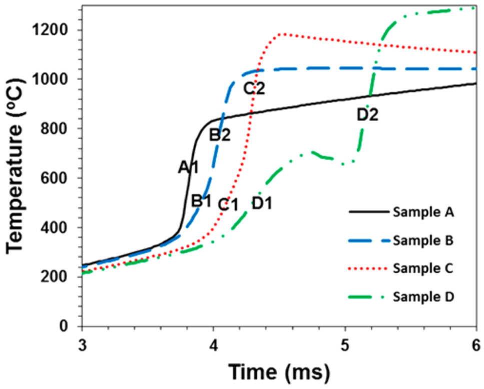

			Stage 1	Stage 2
Sample ID	Sample Thickness	Bilayer Thickness	Avg. Energy Release Rate	Avg. Energy Release Rate
A	199 nm	33 nm	3320 K/ms	-
B	199 nm	66 nm	860 K/ms	2620 K/ms
C	266 nm	66 nm	1030 K/ms	3630 K/ms
D	266 nm	133 nm	610 K/ms	2480 K/ms

Figure 5. Temperature vs time curves for each Al/CuO nanolaminate (samples A–D as listed in Table 1) with labeled reaction stages and corresponding average energy release rates.

to calculate the interface thickness (T_i) and reaction efficiency factor, η, from the theoretical reaction enthalpy (ΔH_{theo}) without premixed interfaces using the results from parallel experiments with the same total thickness, but different number of bilayers as shown in Table 2:

$$\Delta H_{\text{theo}}\eta\frac{(T_t - 2bT_i)}{T_t} = \Delta H_{\text{exp}}$$

where the experimental reaction enthalpy (ΔH_{exp}) is equal to ΔH_{theo} multiplied by the efficiency factor, η, and the fraction of active material in the laminate. The fraction of active material in the laminate is defined as the thickness of active material divided by the total thickness (T_t). The thickness of active material is determined by the total thickness subtracted by two times the number of bilayers (b) times the interface thickness (T_i). For these calculations, the interface is assumed to be fully reacted and therefore does not add energy to the reaction when heated. The ΔH_{theo} for this system is ~−370 kJ/mol CuO. Assuming each laminate has the same T_i and η, respective values of 9.3 nm and 0.31 were calculated. An η of 0.31 means the experimentally determined energy value ~69% is less than the theoretical energy, but our calculations do not take into account the energy required to melt excess Al. As shown above, the MS detects AlO formation during reaction. It is possible that the laminate may be reacting to form a mixture of Al_2O_3 and AlO, which would result in a lower enthalpy of reaction.

Kwon et al. also examined the interface layers of Al/CuO nanolaminates and found the premixed interfacial region to be inhomogeneous with an irregular thickness of up to 5 nm.[14] This value corresponds to a single Al/CuO interface. The calculated premixed interface thickness in Table 2 is almost double this value. The premixed interface thickness was dependent on the deposition temperature. Kwon et al. used a chilled substrate set at 10 °C.[14] For our deposition, the substrate started out at room temperature with sputter deposition causing a slight temperature increase. To deposit Al/CuO onto the nanocalorimeter sensors, good thermal contact between the sensor and sensor holder must be made; otherwise, you would have fully mixed/reacted film with no exothermic signal observed when heated. Poor thermal contact between the sensor and the holder will result in elevated sensor temperatures as the holder acts as a heat sink during deposition. Therefore, the slight temperature increase is most likely the cause for the comparatively larger interface thickness due to the substrate in our study not being chilled.

Two-Stage Reaction Mechanism. Further investigation of the high heating rate temperature vs time data collected from the nanocalorimeter shows a two-stage reaction mechanism for the samples listed in Table 1 with the exception of sample A (six-bilayer, 199 nm total thickness). Linear fits for each reaction regime shown in the temperature vs time plots were used to determine corresponding average energy release rates as seen in Figure 5. Direct heating of the nanocalorimeter by the applied current pulse was approximated to be linear and was deducted from the linear fits during reaction in order to determine the average energy release rates.

For samples B, C, and D, the transition point occurs near the melting point of bulk Al. The first stage of reaction is proposed to be a purely solid-state reaction occurring at the interfaces of Al and CuO. Once the sample is heated to the Al melting point, diffusion rates rapidly increase and gas phase species are then detected by the ToF-MS. Increasing the number of bilayers results in a leftward shift in the second stage of reaction. The second stage of reaction happens earlier due to the increased heat generation caused by the increased interfacial area in the samples with more bilayers. Sample A contains the largest interfacial area and only shows a single reaction step. Due to the large interfacial area and shorter diffusion distance, the solid phase reaction is much faster with an average energy release rate of 3320 K/ms. Furthermore, no endothermic signal was observed from nanocalorimeter data as the temperature reached the melting point of aluminum. Due to the short diffusion distance, the fuel diffusion rate and the fuel supply are sufficient to complete the reaction. As the bilayer thickness/diffusion distance increases, the diffusivities of Al or CuO significantly affect the reaction speed, which is reflected in the observed lower average energy release rate of the first exothermic event for samples with individual bilayer thicknesses greater than 33 nm. A transition in the heating rate occurs around the melting temperature of aluminum for these samples. The Al diffusion rate would be much higher compared to CuO because, after the melting of Al, we did not observe any transition of heating rate, even around the decomposition of CuO in the thickest samples. In addition, by comparing this series of experiments, one may be able to calculate the diffusivities in this thermite system from the heating rate and thickness of the individual layer.

Defining Ignition. Egan et al. have developed a model based on 1D diffusion for nanolaminate ignition that holds true for the samples studied above.[12] The samples studied by Egan et al. were approximately an order of magnitude larger in total thickness than the 199−266 nm-thick samples in Table 1. Table 3 shows measured ignition temperatures using three different experimental methods. The ignition temperature using the optical method is defined as the temperature in which a sharp rise in optical emission taken from high speed video is first observed. The ignition temperature reported in the mass spec method is the onset temperature of detected H_2. The appearance of H_2 marks the start of reaction between Al and any H_2O trapped between the layers of the laminate. This species was used to determine the ignition temperature for the MS method because H_2 has a much higher relative signal intensity than other reaction products detected in the MS. A low relative signal intensity of a product species may result in an overestimate in the onset temperature of said species. The power method for determining the ignition temperature is defined as the onset point of the first exothermic peak after removing the power contribution applied to initially heat the nanocalorimeter sensor.

Table 3. Ignition Temperatures for Each Sample Using High Speed Video, Mass Spectrometry, and Power Data Collected through Nanocalorimetry

				ignition temperature (°C)		
sample ID	sample thickness (nm)	bilayer number	bilayer thickness (nm)	optical method	mass spec. method	power method
A	199	6	33		591	318
B	199	3	66	667	676	319
C	266	4	66	609	661	322
D	266	2	133	697	668	329

In the model reported by Egan et al., the total thickness was 1000 nm and the 12-bilayer sample corresponded to the lowest ignition temperature of ∼350 °C. The experimental ignition temperatures determined by Egan et al. employed the optical method, which was accurate for their system due to the much larger total thickness of their nanolaminates (1800 nm vs 199−266 nm). Their 12-bilayer system corresponds to an approximate bilayer thickness of 150 nm. For our results, sample D in Table 3 has a bilayer thickness of 133 nm and an ignition temperature of ∼330 °C, measured using the power method. This value agrees nicely with the aforementioned 1D diffusion model for nanolaminate ignition.[12] Figure 6 shows the experimentally determined ignition temperatures and iterative ignition model of Egan et al. along with the ignition temperatures measured from our samples as determined by the power method for the Al/CuO nanolaminates listed in Table 3.

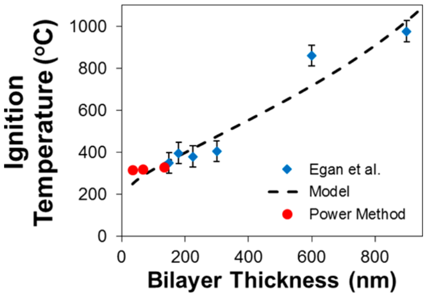

Figure 6. Plot of ignition temperature vs bilayer thickness for experimental values and model by Egan et al. and experimentally calculated values using the power method for Al/CuO nanolaminates in this study.

The power method gives much lower ignition temperatures than both optical and MS methods. The optical method is limited by the sensitivity of the camera and sample size. The heat capacity of the chip is not negligible when the total thickness of the nanolaminate is small resulting in little to no optical emission at the start of reaction. In addition, the MS only detects gas phase products, which may not be released at the earliest stages of ignition. The nanocalorimeter shows an exotherm occurring before any AlO is detected implying that the start of reaction occurs through a condensed phase diffusion based mechanism between the Al and CuO layers. When analyzing the very thin film, as shown in Figure 2, multiple reaction steps are apparent. For the thicker films, there is no heating rate decrease after the initial onset of the exothermic event due to the self-propagation of the reaction. The power method is the only technique, in comparison to mass spectrometry and optical methods, in which the onset temperature of this initial exotherm can be directly measured. We propose that the power method is the most direct method in studying ignition of energetic nanolaminate systems, especially when dealing with small samples and small bilayer thicknesses.

CONCLUSION

By integrating high heating rate chip based calorimetry with ToF-MS, a solid-state initiation was observed for Al/CuO nanolaminates. Samples with an individual bilayer thickness of 33 nm showed a single step reaction mechanism, occurring primarily in the condensed phase, due to this sample showing the highest AlO:Al ratio in the MS. These films demonstrated the highest maximum power output, but lowest overall energy release. The decreased energy release is attributed to the loss of active material in the premixed regions of the interface. The premixed interface thickness was calculated to be 9.3 nm with an efficiency factor of 0.31.

The ignition temperature was measured using optical, MS, and nanocalorimeter based methods and the values compared. Measuring the ignition temperature from the power data collected from the nanocalorimeter proved to be the most accurate method for samples with total thicknesses on the order of hundreds of nanometers. The values measured for the samples in this study showed good agreement with previous Al/CuO nanolaminate ignition models based on their individual bilayer thicknesses.[12]

ASSOCIATED CONTENT

Ⓢ Supporting Information

The Supporting Information is available free of charge on the ACS Publications website at DOI: 10.1021/acs.jpcc.6b11114.

XRD; heating rate and temperature vs time plots; high speed images of Al/CuO (PDF)

AUTHOR INFORMATION

Corresponding Authors

*E-mail: david.lavan@nist.gov.
*E-mail: mrz@umd.edu.

ORCID

Michael R. Zachariah: 0000-0002-4115-3324

Author Contributions

§These authors contributed equally to this work.

Notes

The authors declare no competing financial interest.

■ ACKNOWLEDGMENTS

M.R.Z. and J.B.D. were supported in part by the Army Research Office and DTRA. Certain commercial equipment, instruments, or materials are identified in this document. Such identification does not imply recommendation or endorsement by the National Institute of Standards and Technology, nor does it imply that the products identified are necessarily the best available for the purpose. Nanocalorimeter fabrication was performed in part at the NIST Center for Nanoscale Science & Technology (CNST).

■ REFERENCES

(1) Dreizin, E. L. Metal-based Reactive Nanomaterials. *Prog. Energy Combust. Sci.* **2009**, *35* (2), 141−167.

(2) Rogachev, A. S.; Mukasyan, A. S. Combustion of Heterogeneous Nanostructural Systems (Review). *Combust., Explos. Shock Waves* **2010**, *46* (3), 243−266.

(3) Yetter, R. A.; Risha, G. A.; Son, S. F. Metal Particle Combustion and Nanotechnology. *Proc. Combust. Inst.* **2009**, *32*, 1819−1838.

(4) Blobaum, K. J.; Reiss, M. E.; Plitzko, J. M.; Weihs, T. P. Deposition and Characterization of a Self-propagating CuOx/Al Thermite Reaction in a Multilayer Foil Geometry. *J. Appl. Phys.* **2003**, *94* (5), 2915−2922.

(5) Petrantoni, M.; Rossi, C.; Salvagnac, L.; Conedera, V.; Esteve, A.; Tenailleau, C.; Alphonse, P.; Chabal, Y. J. Multilayered Al/CuO Thermite Formation by Reactive Magnetron Sputtering: Nano Versus Micro. *J. Appl. Phys.* **2010**, *108* (8), 084323.

(6) Rossi, C.; Zhang, K.; Esteve, D.; Alphonse, P.; Tailhades, P.; Vahlas, C. Nanoenergetic Materials for MEMS: A Review. *J. Microelectromech. Syst.* **2007**, *16* (4), 919−931.

(7) Zhang, K.; Rossi, C.; Rodriguez, G. A. A.; Tenailleau, C.; Alphonse, P. Development of a Nano-Al/CuO Based Energetic Material on Silicon Substrate. *Appl. Phys. Lett.* **2007**, *91* (11), 113117.

(8) Rodriguez, G. A. A.; Suhard, S.; Rossi, C.; Esteve, D.; Fau, P.; Sabo-Etienne, S.; Mingotaud, A. F.; Mauzac, M.; Chaudret, B. A Microactuator Based on the Decomposition of an Energetic Material for Disposable Lab-on-Chip Applications: Fabrication and Test. *J. Micromech. Microeng.* **2009**, *19* (1), 015006.

(9) Fu, Y. Q.; Du, H. J.; Huang, W. M.; Zhang, S.; Hu, M. TiNi-based Thin Films in MEMS Applications: A Review. *Sens. Actuators, A* **2004**, *112* (2−3), 395−408.

(10) Rossi, C.; Esteve, D. Micropyrotechnics, a New Technology for Making Energetic Microsystems: Review and Prospective - Review. *Sens. Actuators, A* **2005**, *120* (2), 297−310.

(11) Bahrami, M.; Taton, G.; Conedera, V.; Salvagnac, L.; Tenailleau, C.; Alphonse, P.; Rossi, C. Magnetron Sputtered Al-CuO Nanolaminates: Effect of Stoichiometry and Layers Thickness on Energy Release and Burning Rate. *Propellants, Explos., Pyrotech.* **2014**, *39* (3), 365−373.

(12) Egan, G. C.; Mily, E. J.; Maria, J. P.; Zachariah, M. R. Probing the Reaction Dynamics of Thermite Nanolaminates. *J. Phys. Chem. C* **2015**, *119* (35), 20401−20408.

(13) Michaelsen, C.; Barmak, K.; Weihs, T. P. Investigating the Thermodynamics and Kinetics of Thin Film Reactions by Differential Scanning Calorimetry. *J. Phys. D: Appl. Phys.* **1997**, *30* (23), 3167−3186.

(14) Kwon, J.; Ducere, J. M.; Alphonse, P.; Bahrami, M.; Petrantoni, M.; Veyan, J. F.; Tenailleau, C.; Esteve, A.; Rossi, C.; Chabal, Y. J. Interfacial Chemistry in Al/CuO Reactive Nanomaterial and Its Role in Exothermic Reaction. *ACS Appl. Mater. Interfaces* **2013**, *5* (3), 605−613.

(15) Yi, F.; LaVan, D. A. Electrospray-Assisted Nanocalorimetry Measurements. *Thermochim. Acta* **2013**, *569*, 1−7.

(16) Yi, F.; DeLisio, J. B.; Zachariah, M. R.; LaVan, D. A. Nanocalorimetry-Coupled Time-of-Flight Mass Spectrometry: Identifying Evolved Species during High-Rate Thermal Measurements. *Anal. Chem.* **2015**, *87* (19), 9740−9744.

(17) Swaminathan, P.; Burke, B. G.; Holness, A. E.; Wilthan, B.; Hanssen, L.; Weihs, T. P.; LaVan, D. A. Optical Calibration for Nanocalorimeter Measurements. *Thermochim. Acta* **2011**, *522* (1−2), 60−65.

(18) Swaminathan, P.; LaVan, D. A.; Weihs, T. P. Dynamics of Solidification in Al Thin Films Measured Using a Nanocalorimeter. *J. Appl. Phys.* **2011**, *110* (11), 6.

(19) Zhou, L.; Piekiel, N.; Chowdhury, S.; Zachariah, M. R. T-Jump/Time-of-Flight Mass Spectrometry for Time-Resolved Analysis of Energetic Materials. *Rapid Commun. Mass Spectrom.* **2009**, *23* (1), 194−202.

(20) Jian, G.; Piekiel, N. W.; Zachariah, M. R. Time-Resolved Mass Spectrometry of Nano-Al and Nano-Al/CuO Thermite under Rapid Heating: A Mechanistic Study. *J. Phys. Chem. C* **2012**, *116* (51), 26881−26887.